Eur Phys J A (2005) **24,** s1, 143–147
DOI: 10.1140/epjad/s2005-05-025-7

EPJ A direct
electronic only

Spin asymmetries for confined Dirac particles

M.W. Paris[1], V.R. Pandharipande[2], and I. Sick[3]

[1] Thomas Jefferson National Accelerator Facility, MS12H2, 12000 Jefferson Ave, Newport News, VA, 23606, USA
[2] Department of Physics, University of Illinois at Urbana-Champaign, Urbana, Illinois 61801, USA
[3] Departement für Physik und Astronomie, Universität Basel, Switzerland

Received: 27 September 2004 / Published Online: 8 February 2005

Abstract. We study the Bjorken x (or equivalently Nachtmann ξ) dependence of the virtual photon spin asymmetry in polarized deep inelastic scattering of electrons from hadrons. We use an exactly solved relativistic potential model of the hadron, treating the constituents as independent massless Dirac particles confined to an infinitely massive force center. The importance of including the p–wave components of the Dirac wave function is demonstrated. Comparisons are made to the observed data on the proton by taking into account the observed flavor dependence of the valence quark distribution functions.

PACS. 13.60.Hb Photon and charged-lepton interactions with hadrons – 12.39.Ki Relativistic quark model – 12.39.Pn Potential model

1 Introduction

The structure functions of the nucleon as measured by deep inelastic scattering (DIS) of leptons from nucleons have, over the last 30 years, received much attention. In particular, the evolution with momentum transfer Q^2 has been quantitatively understood in terms of quantum chromodynamics (QCD).

During the last decade, the interest has been concentrated on the *spin structure functions*. Much of this interest was due to the fact that the integral over the experimental spin structure function $g_1(x)$ yielded values that were much lower than the ones expected in the naive quark model (for reviews see e.g. [1,2,3]). The presence of this "spin crisis" has led to many different ideas on how to account for the nucleon spin. The contribution of $s\bar{s}$-components, the contribution of orbital angular momenta of the quarks and the contribution of gluons have been discussed. It also has been pointed out early on [4] that the non-relativistic quark model overestimates the quark contribution to the nucleon spin. Relativistic effects lead to a reduction which today, together with the gluon contribution via the triangle diagram, are believed to provide the main explanation for the low integral over the spin structure function g_1; in the present letter, we concentrate on the former.

Relativistic effects are expected to play an important role as the masses of quarks are small compared with their momenta. The non-relativistic quark models for instance also overestimate the axial vector weak coupling constants which experimentally amount to $g_A/g_V = 1.26$ rather than 5/3. Calculations with the MIT bag model [5] or using light-cone quantization [6] have indicated that the lower components of the wave function — present in a relativistic description using the Dirac equation — lead to an opposite contribution to the one of the upper components, which could generate, in the limit of massless quarks, a reduction factor of 0.65 [7].

The present calculation is similar to bag model calculations in [8,9,10,11]. In these works the struck constituent was treated as a free particle whose state is therefore described by a plane wave. Here we use an exacly solved single particle relativistic potential model of the hadron. The state of the struck constituent is described by the *eigenstates* of this Hamiltonian which are four-component Dirac spinors.

The main purpose of the present work is to clarify the role of the (lower component) $p-$wave terms of the ground state Dirac wave function in determining the x dependence of the $g_1(x)$. The interference between the dominant $s-$wave and the smaller $p-$wave parts of the valence quark Dirac wave function is shown to suppress $g_1(x)$ at small values of x. This novel observation demonstrates in an unambigous way an effect of treating hadronic constituents as bound Dirac particles.

2 Virtual photon longitudinal asymmetry

2.1 Model calculation

We consider the calculation of the virtual photon spin asymmetry in DIS of a charged leptonic probe from a hadronic target within the model of [12]. The Hamiltonian in this model is chosen as

$$H = \boldsymbol{\alpha}\cdot\mathbf{p} + \frac{1+\beta}{2}\sqrt{\sigma}r, \tag{1}$$

where $\boldsymbol{\alpha}$ and β are Dirac matrices in the standard representation [13]. It describes a massless Dirac particle in a linear confining well. The half-vector plus half-scalar structure of the confining potential is chosen for its spin symmetry [14] wherein spin-orbit doublets are degenerate. It is motivated by the relatively small spin-orbit splittings seen in meson spectra. Computations are simple with this choice since the lower components of the wave function are not coupled by the potential. The value of the string tension $\sqrt{\sigma}$ is assumed to be 1 GeV/fm as indicated by the slopes of baryon Regge trajectories. In [12] all the eigenstates of this model were obtained exactly for excitation energies up to ~ 12 GeV. The ground state energy, E_0 for this string tension is 840 MeV. The model may be viewed as a heavy-light meson, such as $\bar{t}u$, in the limit that the antiquark mass goes to infinity. However, it retains only the confining part of the $\bar{t}u$ interaction modeled by a flux tube.

The model neglects gluon and sea-quark contributions to DIS as well as the QCD evolution. However, the observed ratio of the $g_1(x)$ to $F_1(x)$, the unpolarized structure function is relatively independent of Q^2 [1], and our objective is to calculate the x-dependence of this ratio for the contribution of valence quarks to DIS. We hope that the model is useful in this context.

The virtual photon asymmetry is defined as [1]

$$A_1 = \frac{\sigma_{\frac{1}{2}} - \sigma_{\frac{3}{2}}}{\sigma_{\frac{1}{2}} + \sigma_{\frac{3}{2}}} \tag{2}$$

with $\sigma_{\frac{1}{2}}$ and $\sigma_{\frac{3}{2}}$ the helicity cross sections for the target angular momentum antiparallel and parallel to the photon helicity, respectively. We may calculate the inclusive virtual photon helicity cross sections in the rest frame of the target as

$$\sigma_{\frac{1}{2}}(|\mathbf{q}|,\nu) = \sigma_M \sum_I \left|\langle I|\alpha_+ e^{i|\mathbf{q}|z}|0,-\tfrac{1}{2}\rangle\right|^2 \delta(E_I - E_0 - \nu) \tag{3}$$

$$\sigma_{\frac{3}{2}}(|\mathbf{q}|,\nu) = \sigma_M \sum_I \left|\langle I|\alpha_+ e^{i|\mathbf{q}|z}|0,+\tfrac{1}{2}\rangle\right|^2 \delta(E_I - E_0 - \nu) \tag{4}$$

where $|\mathbf{q}|$ and ν are the momentum and energy transferred to the target, σ_M is the Mott cross section and we have assumed that the virtual photon is in the $\hat{\mathbf{z}}$ direction. The ground states $|0, j_z = \pm\frac{1}{2}\rangle$ have the total angular momentum projection $j_z = \pm\frac{1}{2}$. The operator α_+ corresponds to a virtual photon with positive helicity, and $|I\rangle$ are eigenstates of the Hamiltonian H (1) with energies E_I.

The calculation of the virtual photon helicity cross sections proceeds in this model, without approximations, exactly as the calculation of the unpolarized structure functions described in [12]. When $|\mathbf{q}|$ is large the σ/σ_M depend only on $\tilde{y} = |\mathbf{q}| - \nu$. Figure 1 shows the calculated $\sigma_{\frac{1}{2}}/(2\sigma_M)$ and $\sigma_{\frac{3}{2}}/(2\sigma_M)$ plotted as a function of the scaling variable $\tilde{y}$, and their sum

$$F_1^q(\tilde{y}) = \frac{1}{2\sigma_M}\left(\sigma_{\frac{1}{2}} + \sigma_{\frac{3}{2}}\right), \tag{5}$$

the unpolarized structure function. The conventionally used Bjorken and Nachtmann scaling variables are related

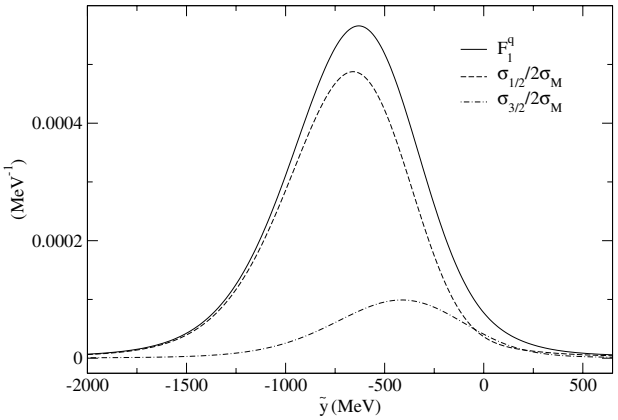

Fig. 1. Virtual photon helicity cross section of a confined massless quark, modulo twice the Mott cross section, as a function of $\tilde{y}$. The *dashed* ($\sigma_{\frac{1}{2}}$) and *dash-dotted* ($\sigma_{\frac{3}{2}}$) curves sum to the unpolarized structure function (*solid curve*)

to $\tilde{y}$ by [15]:

$$x(Q^2 \to \infty) = \xi = -\frac{\tilde{y}}{M_T}, \tag{6}$$

where M_T is the target mass. Thus small (large) negative $\tilde{y}$ correspond to small (large) x. We note that the $\sigma_{\frac{1}{2}}(\tilde{y})$ and $\sigma_{\frac{3}{2}}(\tilde{y})$ are not proportional, which implies that the A_1^q of a confined relativistic quark has a large $\tilde{y}$ or equivalently x dependence.

The ground state $|0, j_z\rangle$ of the confined quark is given by:

$$\Psi_{0,j_z}(\mathbf{r}) = \begin{pmatrix} f_0(r)\mathcal{Y}^0_{\frac{1}{2},j_z}(\hat{\mathbf{r}}) \\ ig_0(r)\mathcal{Y}^1_{\frac{1}{2},j_z}(\hat{\mathbf{r}}) \end{pmatrix}, \tag{7}$$

where, $f_0(r)$ and $g_0(r)$ are the radial functions for the s– and p–waves, respectively, and $\mathcal{Y}^\ell_{j,j_z}$ are the spin-angle functions obtained by coupling spin and orbital angular momentum to $j = \frac{1}{2}$.

The interference in the DIS between the s– and p–waves contributes significantly to the $\tilde{y}$ dependence of the $\sigma_{\frac{1}{2}}$ helicity cross-section, A_1^q and F_1^q. The effect of interference is shown in Fig. 2 where we compare the polarized cross section $\sigma_{\frac{1}{2}}$ including interference terms (solid curve, labeled 'full') with the polarized cross section neglecting interference terms (dotted curve). Also shown are the polarized cross sections obtained after keeping only the s– or p–waves in the $j_z = -\frac{1}{2}$ target. We note that the interference shifts $\sigma_{\frac{1}{2}}$ to more negative $\tilde{y}$ corresponding to larger values of ξ. Only the p–waves contribute to $\sigma_{\frac{3}{2}}$ shown in Fig. 1.

The virtual photon asymmetry is given in terms of the spin-dependent structure functions g_1 and g_2 [1] by

$$A_1 = \frac{g_1 - \gamma^2 g_2}{F_1} \approx \frac{g_1}{F_1} \tag{8}$$

where $\gamma^2 = 4M_T^2x^2/Q^2$, in the scaling regime, $Q^2 \to \infty$. As mentioned earlier, the observed A_1 of the proton, A_1^p

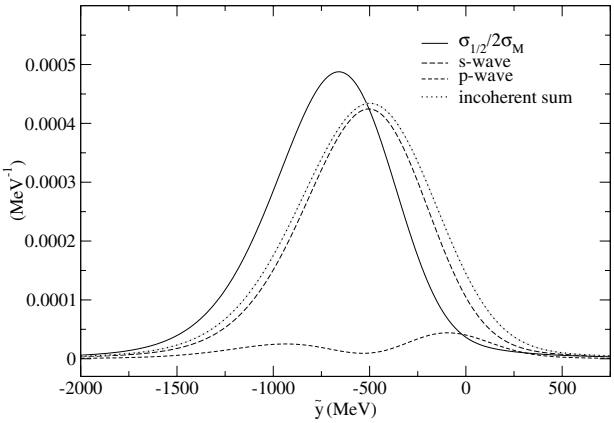

Fig. 2. Interference effects in $j_z = -\frac{1}{2}$ ($\sigma_{\frac{1}{2}}$) structure function. The *dashed lines* give the contributions of the s- and p-waves alone, the *dotted line* shows their incoherent sum and *full line* is the exact result

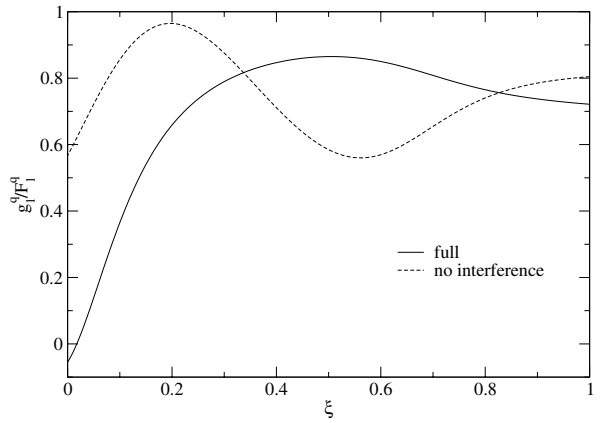

Fig. 3. The g_1^q/F_1^q for a single massless quark confined by a flux-tube, as a function of the Nachtmann $\xi = (|\mathbf{q}| - \nu)/M_T$ with and without interference terms (see text)

is largely independent of Q^2, and is used to extract values of g_1^p/F_1^p [1].

Using the structure functions given in Fig. 1 we can easily calculate the virtual photon asymmetry A_1^q or equivalently the ratio g_1^q/F_1^q for a single confined quark, as a function of $\tilde{y}$. In order to compare it with the data on protons we have to convert it to a function of ξ by providing a mass scale M_T (see (6)). Our model target has infinite mass associated with the center of the confining potential. However, that mass is not relevant since only the confined quark contributes to DIS. We use $M_T = 2.5$ GeV $\sim 3E_0$, where E_0 is the energy of a single confined quark in the ground state. With this choice the $F_1^q(\xi)$ becomes small at $\xi \sim 0.8$ as in the proton. The fact that the model target has infinite mass means that response can be non-zero, in principle, at arbitrarily large values of $\xi > 0$. In fact the calculated structure functions shown in Figs. 1 and 2 are very close to zero at $\tilde{y} = -2000$ MeV corresponding to $\xi \approx 0.8$. Nevertheless, the present model should not be used for values of $\xi \gtrsim 0.8$.

The solid curve in Fig. 3 shows the $A_1^q(\xi)$ or equivalently $g_1^q(\xi)/F_1^q(\xi)$ of a confined quark. The calculated ratio goes to zero at small ξ, and this behavior is independent of the chosen value of M_T. The dip at $\xi = 0$ is due to the shift of $\sigma_{\frac{1}{2}}$ to larger values of ξ, produced by the interference effect shown in Fig. 2. When the interference terms are omitted we obtain the dashed curve in Fig. 3 which has $g_1^q/F_1^q \sim 0.6$ at $\xi = 0$.

Alternatively we could have chosen the string tension $\sqrt{\sigma}$ such that $3E_0 = M_N$, the nucleon mass. However, since $\sqrt{\sigma}$ provides the only mass scale in the Hamiltonian H (1), this choice gives exactly the same $A_1^q(\xi)$ as the previous.

2.2 Comparison to observed asymmetry in proton

We have, up to this point, presented our exact calculation of the spin asymmetry, $A_1^q(\xi)$ for a single confined quark in terms of the eigenstates of the single particle Hamiltonian, (1). We have made the novel observation that the suppression at small ξ is a consequence of $s-$ and $p-$wave interference terms. One would like, however, to compare the predictions of the present model with the observed spin asymmetry of the nucleons. In the remaining parts of this letter we attempt to estimate the ξ dependence of g_1^p/F_1^p ratio for the proton in the "naive" quark model in which the total PDF (parton distribution functions) are approximated by the sum of the three valence quark contributions. We apply the analysis of [16] to incorporate the flavor dependence of the PDF's. The unpolarized PDF of valence quarks in $j_z = \pm\frac{1}{2}$ states are denoted by $u(\pm\frac{1}{2}, \xi)$ and $d(\pm\frac{1}{2}, \xi)$. They correspond to those obtained from the MRST [17] PDF fits to the experimental data. The asymmetry $A_1^q(\xi)$ calculated above for a confined quark is used together with these experimental unpolarized distribution functions to estimate the g_1^p/F_1^p.

In order to obtain the asymmetry of the proton we must account for the flavor dependence of the PDF's, as extracted from experiment. It is well known that the flavor dependence of the valence PDF's can be understood in terms of the state of the residual system after removal of the struck quark [16,15]. The residual diquark in DIS from protons can be in a spin-0 or spin-1 state. Removal of a d quark results in a spin-1 diquark, while removal of a u quark results in a spin-0 diquark 3/4 of the time and spin-1 for the remainder.

Let $q_0(\xi)$ and $q_1(\xi)$ be the unpolarized PDF when the diquark is in spin-0 and 1 state respectively. From the proton spin-flavor wave function we obtain

$$\begin{aligned} u(+\tfrac{1}{2}, \xi) &= \frac{3}{2} q_0(\xi) + \frac{1}{6} q_1(\xi) \\ u(-\tfrac{1}{2}, \xi) &= d(+\tfrac{1}{2}, \xi) = \frac{1}{3} q_1(\xi) \\ d(-\tfrac{1}{2}, \xi) &= \frac{2}{3} q_1(\xi). \end{aligned} \tag{9}$$

The empirically known, total unpolarized $u(\xi)$ and $d(\xi)$ are given by

$$u(\xi) = u(+\tfrac{1}{2}, \xi) + u(-\tfrac{1}{2}, \xi)$$

$$= \frac{3}{2}q_0(\xi) + \frac{1}{2}q_1(\xi)$$
$$d(\xi) = d(+\tfrac{1}{2},\xi) + d(-\tfrac{1}{2},\xi) = q_1(\xi). \quad (10)$$

Solving the above equations for $q_0(\xi)$ and $q_1(\xi)$ using the MRST [17] $u(\xi)$ and $d(\xi)$ we find that q_0 is shifted to larger values of ξ with respect to q_1 as expected from the smaller mass of the spin-0 diquark. Eliminating q_0 and q_1 from (9) and (10) we obtain:

$$u(+\tfrac{1}{2},\xi) = u(\xi) - \frac{1}{3}d(\xi)$$
$$u(-\tfrac{1}{2},\xi) = d(+\tfrac{1}{2},\xi) = \frac{1}{3}d(\xi)$$
$$d(-\tfrac{1}{2},\xi) = \frac{2}{3}d(\xi). \quad (11)$$

Due to the presence of p–waves both the $j_z = \pm\frac{1}{2}$ PDF's have spin $\uparrow$ and $\downarrow$ contributions. In principle we need the spin asymmetries of the $q_0(\xi)$ and $q_1(\xi)$ distributions to obtain the spin dependent PDF's. Here we approximate both of them by the spin asymmtery $A_1^q(\xi)$ of a quark in the $j = \frac{1}{2}$ ground state of a linear confining potential, calculated above and shown in Fig. 3. For example the $u(j_z,\xi)$ are given by:

$$u_\uparrow(\pm\tfrac{1}{2},\xi) + u_\downarrow(\pm\tfrac{1}{2},\xi) = u(\pm\tfrac{1}{2},\xi) \quad (12)$$
$$u_\uparrow(\pm\tfrac{1}{2},\xi) - u_\downarrow(\pm\tfrac{1}{2},\xi) = \pm A_1^q(\xi)u(\pm\tfrac{1}{2},\xi). \quad (13)$$

The total spin $\uparrow,\downarrow$ PDF's, summed over j_z, are obtained from the above equations. They are given by:

$$u_{\uparrow,\downarrow}(\xi) = \frac{u(\xi)}{2}\left[1 \pm A_1^q(\xi)\right] \mp \frac{d(\xi)}{3}A_1^q(\xi) \quad (14)$$
$$d_{\uparrow,\downarrow}(\xi) = \frac{d(\xi)}{2}\left[1 \mp \frac{1}{3}A_1^q(\xi)\right], \quad (15)$$

We may now compute the spin asymmetry in the proton. Using

$$F_1(\xi) = \frac{1}{2}\left[\frac{4}{9}u(\xi) + \frac{1}{9}d(\xi)\right] \quad (16)$$
$$g_1(\xi) = \frac{1}{2}\left[\frac{4}{9}\left(u_\uparrow(\xi) - u_\downarrow(\xi)\right) + \frac{1}{9}\left(d_\uparrow(\xi) - d_\downarrow(\xi)\right)\right], \quad (17)$$

and obtain

$$\frac{g_1^p(\xi)}{F_1^p(\xi)} = \left(\frac{4u(\xi) - 3d(\xi)}{4u(\xi) + d(\xi)}\right)A_1^q(\xi). \quad (18)$$

This ratio is plotted in Fig. 4 as the solid curve and is in fair agreement with the data from [1] at all ξ. The PDF's evolved to $Q^2 = 5$ GeV^2 at next-to leading order are used to obtain the results shown in Fig. 4, but the ratio, $(4u(\xi) - 3d(\xi))/(4u(\xi) - d(\xi))$ is fairly insensitive to Q^2 in the range $2 < Q^2 < 20$ GeV^2.

It should be pointed out that at $\xi < 0.2$ the sea quark contributions to the $F_1^p(\xi)$ are large, particularly at large Q^2. However, they are neglected in the present calculation.

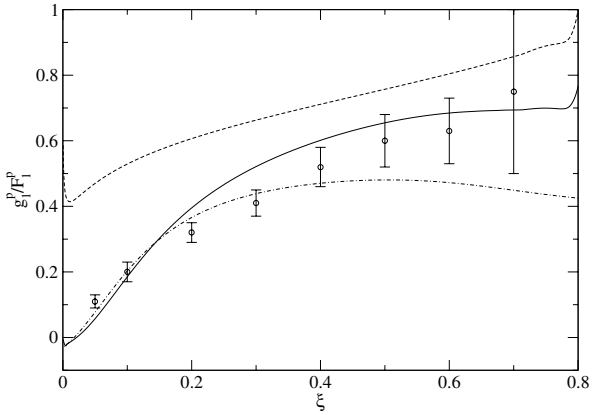

Fig. 4. The g_1^p/F_1^p from MRST $u(\xi)$ and $d(\xi)$. The *full line* shows results obtained with the calculated A_1^q while the *dashed line* shows results assuming $A_1^q = 1$. The *dash-dot line* is obtained using the approximation $u(\xi) = 2d(\xi)$. The data is from [1]

If we neglect p–waves in the valence quark orbitals, then $A_1^q(\xi) = 1$. The resulting g_1^p/F_1^p is significantly above the experimental data as shown in Fig. 4. In the $SU(6)$ limit of the naive quark model we have $u(\xi) = 2d(\xi)$ and (18) reduces to

$$\frac{g_1^p(\xi)}{F_1^p(\xi)} = \frac{5}{9}A_1^q(\xi). \quad (19)$$

Results obtained with this approximation are shown by the dot-dashed curve in Fig. 4. It lies below the data at large ξ. Approximating the A_1^q by unity in the above equation gives the ξ independent result, $g_1^p/F_1^p = 5/9$, of Kuti and Weisskopf [18].

3 Conclusion

In conclusion the present work suggests that at least two different effects shape the ξ dependence of $A_1^p(\xi)$. The p–waves in bound quark wave functions interfere with the dominant s-waves to suppress $A_1^q(\xi)$ at small ξ; and the difference in the shapes of the $u(\xi)$ and $d(\xi)$ enhances the $A_1^p(\xi)$ at large ξ.

Our model is certainly too simple; it approximates the problem of three interacting quarks by a relativistic one-quark problem. Nevertheless p–waves occur very naturally in the wave functions of spin-half relativistic particles, and their effect will presumably exist in more refined treatments of spin asymmetries.

Acknowledgements. This work has been supported by the US National Science Foundation via grant PHY-00-98353, and by the US Department of Energy under contract W-7405-ENG-36 and the Schweizerische Nationalfonds.

References

1. B. Filippone, X. Ji: The spin structure of the nucleon, Adv. Nucl. Phys. **26**, 1 (2001)

2. M. Anselmino, A. Efremov, E. Leader: The theory and phenomenology of polarized deep inelastic scattering, Phys. Rep. **261**, 1 (1995)
3. E.W. Hughes, R. Voss: Spin structure functions, An. Rev. Nucl. Part. Sci. **49**, 303–339 (1999)
4. J.D. Bjorken: Applications of the chiral $U(6)\otimes U(6)$ algebra of current densities, Phys. Rev. **148**, 1467 (1966)
5. R.L. Jaffe: g_2: The nucleon's other spin-dependent structure function, Comm. Nucl. Part. Phys. **14**, 239 (1990)
6. S.J. Brodsky, F. Schlumpf: Wave function independent relations between the nucleon axial coupling g_A and the nucleon magnetic moments, Phys. Lett. B **329**, 111–116 (1994)
7. R.L. Jaffe, A. Manohar: The g_1 problem: fact and fantasy on the spin of the proton, Nucl. Phys. B **337**, 509–546 (1990)
8. R.L. Jaffe, Deep inelastic structure functions in an approximation to the bag theory, Phys. Rev. D **11**, 1953 (1975)
9. A.W. Schreiber, A.I. Signal, A.W. Thomas: Structure functions in the bag model, Phys. Rev. D **44**, 2653 (1991)
10. R.L. Jaffe, X. Ji: Chiral-odd parton distributions and Drell-Yan processes, Nuc. Phys. B **375**, 527 (1992)
11. X. Song, J.S. McCarthy: Model calculation of nucleon structure functions, Phys. Rev. D **49**, 3169–3186 (1994)
12. M.W. Paris, Electromagnetic response of confined Dirac particles, Phys. Rev. C **68**, 025201 (2003)
13. J. Bjorken, S. Drell: *Relativistic Quantum Mechanics* (McGraw-Hill Book Co., 1964)
14. P.R. Page, T. Goldman, J.N. Ginocchio: Relativistic symmetry suppresses quark spin-orbit splitting, Phys. Rev. Lett. **86**, 204–207 (2001)
15. O. Benhar, V.R. Pandharipande, I. Sick: Many-body theory interpretation of deep inelastic scattering, Phys. Lett. B **489**, 131–136 (2000)
16. F.E. Close, A.W. Thomas: The spin and flavor dependence of parton distribution functions, Phys. Lett. B **212**, 227 (1988)
17. A.D. Martin, R.G. Roberts, W.J. Stirling, R.S. Thorne: Uncertainties of predictions from parton distributions. I: Experimental errors, Eur. Phys. J. C **28**, 455–473 (2003)
18. J. Kuti, V.F. Weisskopf: Inelastic lepton-nucleon scattering and lepton pair production in the relativistic quark-parton model, Phys. Rev. D **4**, 3418 (1971)